PHYSICAL REVIEW D VOLUME 24, NUMBER 9 1 NOVEMBER 1981

Topological supersymmetric structure of hadron cross sections

P. Gauron, B. Nicolescu, and S. Ouvry
Division de Physique Théorique, Institut de Physique Nucléaire, 91406 Orsay, France*
and Laboratoire de Physique Théorique des Particules Elémentaires, Université Pierre et Marie Curie, Paris, France
(Received 26 May 1981)

A way of fully implementing unitarity and confinement in the framework of a dual-topological-unitarization theory, including not only mesons but also baryons, has recently been found. This theory consists in the topological description of hadron interactions in terms of two two-dimensional surfaces (a closed "quantum" surface and a bounded "classical" surface). We show that this description directly leads, at the zeroth order of the topological expansion, to certain relations between hadron cross sections, in nice agreement with experimental data. A new topological suppression mechanism is shown to play an important dynamical role. We also point out a new topological supersymmetry property, which leads to realistic experimental consequences. A possible topological origin of the ρ and ω universality relations emerges as a by-product of our study.

I. INTRODUCTION

It is well known that dual topological unitarization[1] (DTU) is a promising approach to S-matrix theory, which attempts to calculate hadron spectroscopy and scattering using only crossing and unitarity, and the maximal analyticity consistent with these properties. This approach, which is particularly suitable for small momentum transfers (and hence large distances), can be regarded as a way of dealing with quark confinement. In this sense, the DTU approach appears to be complementary to the perturbative quantum-chromodynamics (QCD) theory, which nicely describes large-momentum-transfers physics.

The DTU program involves two stages:

(i) In the lowest order of the topological expansion one assumes that the full amplitude $\mathcal{T}$ can be written as a linear combination of a set of "ordered" amplitudes T with simpler properties. Namely, they satisfy simple crossing properties and also a form of reduced unitarity, which does not incorporate exchange effects. If we now combine this reduced unitarity and crossing with maximal analyticity, we are led to a system of self-consistent (bootstrap) equations, whose solution would give a lowest-order hadron spectrum. It is important to note that in the zeroth order of the topological expansion, duality appears as an *exact* property (topologists give the name "the Whitehead move" to the transformation which physicists refer to as "the duality property").

(ii) In higher orders of the topological expansion one brings in exchange effects through a topological expansion. All higher-order contributions are systematically computed from the zeroth-order contribution. The topological complexity index defines the meaning of "higher orders". It must possess an "entropy" property: under any unitarity product either it stays stationary or it increases. An "order relation" can be so defined. The assumed convergence of the topological expansion ensures that more complex, "disordered" contributions are suppressed when compared with simpler, "ordered" contributions. DTU can thus be viewed as an S-matrix topological perturbation theory, which incorporates (and even requires) a given quarklike structure of hadrons.

The DTU approach to hadron physics is quite successful in the case of the mesons.[1] However, its extension to the baryons is intrinsically difficult, because of the complex nature of the topological complexity index which governs the topological expansion. For several years, no way was found for fully satisfying any kind of reduced unitarity at the lowest level.

Recently, important progress has been made in this direction. This has led to the necessity of considering a new "quantum surface"[2,3] which is conceived as the source of the internal quantum numbers and is responsible for confinement. This new topological variety has to be considered in addition to the "classical surface" which describes the space-time structure of hadron collisions.[4] An important step forward has been the elaboration of a coherent method for incorporating spin into the topological expansion.[5]

Finally, a complete topological expansion theory, involving both the "classical" and "quantum" surfaces, has been formulated.[6] An interesting novel feature of the theory of Ref. 6 is the explicit embedding of the Landau unitarity graphs on the classical surface, which now appear in addition to the familiar Harari-Rosner graphs.[7] The rich topological content of the theory allows the tackling of questions such as the following: Why is there a confinement of quarks? Why are there three colors? Why is there a limited number of flavors? At the same time it provides a firm context for computing hadron observables in a region

where the confinement phenomenon is fully relevant.

In this paper we want to show that the lowest-entropy level of the theory is able to determine a great deal of physics for an important class of phenomena. Namely, we apply the DTU formalism to the study of hadron total and inclusive cross sections and discover that many empirical regularities, some of them known for a long time,[8] seem to have a general topological foundation. A new topological suppression mechanism, which appears as a consequence of the inclusion of Landau graphs on the classical surface, is shown to play an important dynamical role. Moreover, we show that the topological amplitudes satisfy a "supersymmetry" property, which leads to consequences which are in agreement with the data.

A short summary of the features of the new DTU theory (including baryons)[6] which are relevant for this paper, is made in Sec. II. The supersymmetry property of the topological amplitudes relating bosons to fermions is derived in Sec. III. The topological supersymmetric structure of hadron cross sections is discussed in Sec. IV and compared with the experimental data in Sec. V. An interesting consequence of this topological structure for Regge couplings is shown in Sec. VI. Conclusions are drawn in Sec. VII.

II. SHORT DESCRIPTION OF THE GENERAL DTU FRAMEWORK

Hadron interactions are described in the theory of Ref. 6 by a pair of surfaces, a quantum surface and a classical surface. The quantum surface is two-dimensional, orientable, and closed. The last property is related to the conservation of internal quantum numbers. The quantum surface is the space of *structures*, the space of confined constituents. The classical surface is, like the quantum surface, two-dimensional and orientable. Its distinctive feature is the fact that it is bounded and multisheeted. The boundary of the classical surface is obtained via its intersection with the quantum surface. This intersection (the "belt"[6]) leads to graphs which are very similar to the familiar Harari-Rosner graphs.[7] However, the quark lines of these new graphs describe neither the flow of the energy-momentum of the quarks nor their flavors, but are consistently associated with $\pm\frac{1}{2}$-spin indices of the quarks.[5] The space-time aspects of hadron collisions are described by Landau graphs embedded on the classical surface, each Landau arc being associated with the energy-momentum four-vector of a particle.

A basic achievement of the theory of Ref. 6 is the rigorous mathematical definition of a topological complexity index which possesses the previously mentioned "entropy" property: Under any unitarity product either it stays stationary or it increases. A given set of fixed values of the indices which enter into the structure of the topological complexity index determines a given allowed surface pair, up to a *finite* number of possible choices. The theory is thus perfectly defined at any given order of the topological expansion.

A proper mathematical definition of the overall topological entropy index involves a triangulation of the quantum surface. The triangle—the two-dimensional simplex—appears naturally as the "basic" object of the present construction.

The fundamental, "primordial" level of the topological expansion is the zero-entropy level, where the nonlinearity of the bootstrap problem is concentrated.[6] The definition of hadrons has to be made at this lowest entropy level. All higher orders have to be obtained via appropriate connected sums (i.e., unitarity products) of the zero-entropy amplitudes.

At zero entropy the quantum surface is a sphere and the classical surface is a multiplane surface with a "three-feathered" structure (i.e., can be expressed through connected sums of an appropriate succession of three bounded planes intersecting along a "junction line"). The Landau graph is a univertex graph and is located on the classical surface.

At the same zero-entropy level, the particles are represented by "discs," i.e., by bounded regions of the quantum sphere without topological singularity points (in simpler words, a disc is a region of the sphere whose perimeter touches itself only once). The perimeter of a disc gives the "identity" of a hadron, being a representation of flavor indices, while the interior of a disc has to be related to color indices.

It is important to note the close relationship between the notion of disc and the notion of "multiparticle channel resonance." Namely, the topological contraction of any collection of discs belonging to a given sector (or channel) of the "spherical" (or ordered) Hilbert space leads *uniquely* to a given particle disc. In other words, the particles belonging to that channel resonate. Here one can find the very root of the potential physical mechanism controlling the convergence of the topological expansion.

Now, the hadrons are represented in the following way. A meson is represented by a four-edge disc consisting of two "peripheral triangles" [Fig. 1(a)], a baryon is represented by a six-edge disc consisting of three peripheral triangles surrounding a "core triangle" [Fig. 1(b)], and a baryonium is represented by an eight-edge disc consisting of

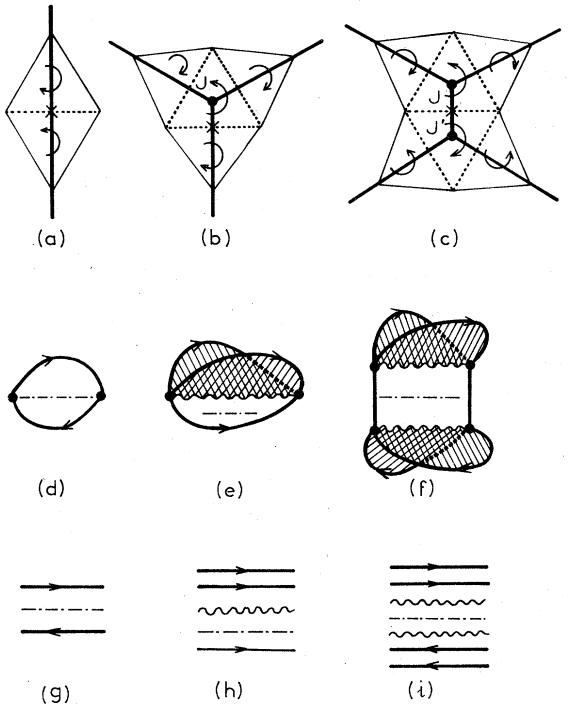

FIG. 1. (a)–(c) Meson, baryon, and baryonium discs on the quantum surface. The heavy solid lines represent the traces left by the corresponding intersection between the classical surface and the quantum surface (in other words they represent the segments of the overall "belt"). The crosses denote the ends of Landau arcs and the points J denote the ends of junction lines. (d)–(f) The classical surfaces corresponding to the propagators of the particles shown in (a)–(c). The dashed-dotted lines denote Landau arcs and the wiggly lines denote junction lines. (g)–(i) Hadron propagators in a Harari-Rosner form, obtained by "opening" the vertices in (d)–(f).

four peripheral triangles surrounding two core triangles [Fig. 1(c)]. We call here "peripheral triangles" the triangles which have a trivial vertex (i.e., a vertex which joins only two edges). It is seen from Figs. 1(b) and 1(c) that the core triangles have no trivial vertex. All trivial vertices lie on the disc perimeters. The orientations of the triangles correspond to an overall patchwise orientation of the quantum sphere[6] (any two contiguous triangles in a given triangulation pattern, which share at least one edge, have opposite orientations).

The peripheral triangles describe the topological flavor of the quarks (e.g., by attaching orientations on their edges one obtains eight possible topological flavors).[6] The orientations of the interiors of the peripheral triangles distinguish between quarks and antiquarks. The peripheral triangles are not discs—they have incomplete boundaries. Therefore, they cannot appear as physical states. The topological quarks are, by construction, confined. It is important to remember that flavor resides on the quantum surface, not on the classical surface.

On the classical surface, a meson is represented by a bounded plane as in Fig. 1(d), a baryon by three bounded planes intersecting along a junction line [Fig. 1(e)] and a baryonium by five bounded planes and two junction lines [Fig. 1(f)]. (These representations are somewhat similar to those considered by Rossi and Veneziano[9] in a different context.) It is easy to verify that by covering the quantum sphere with one of the particles of Figs. 1(a)–1(c) and its corresponding antiparticle and intersecting it with the associated classical surface one obtains as "belt" precisely the boundary of the corresponding topological form shown in Figs. 1(d)–1(f). By "opening" the vertices of Figs. 1(d)–1(f) and by an appropriate projection onto a plane one obtains the meson, baryon, and baryonium propagators in their usual Harari-Rosner form [Figs. 1(g)–1(i)], supplemented, of course, with Landau arcs (one per particle) and junction lines (0 for mesons, one for baryons, and two for baryonia). As we already discussed in the Introduction, the quark lines of Figs. 1(d)–1(f) or of Figs. 1(g)–1(i) are associated with the spin indices of the quarks.

The consistency of the theory imposes the following alternative: either the spectrum of hadrons consists of only ordinary mesons, ordinary baryons, and baryonia or one has to start new bootstrap cycles, involving additional multiquark hadrons which are completely stable at zero entropy (i.e., a single particle of this kind does not couple to the particles defined in Fig. 1; their nonzero coupling would involve intersections between Landau lines and junction lines, which are forbidden at zero entropy). We adopt here, for simplicity, the attitude of Ref. 6, i.e., we choose the first case: the hadron spectrum stops at the baryonium level. However, the results presented in our paper do not depend on this choice.

In order to illustrate the above general considerations let us consider the simplest hadron amplitude: the elastic meson-meson amplitude. This amplitude corresponds to the pair of two-dimensional surfaces shown in Fig. 2(a). The quantum surface is the surface of the sphere of Fig. 2(a) covered by four mesons of the type shown in Fig. 1(a), i.e., by eight triangles ("topological quarks" or "topological antiquarks"). It is obviously patchwise oriented. The classical surface is the equatorial plane of the sphere in Fig. 2(a). It contains a univertex Landau graph, the Landau lines terminating at the quantum sphere. The belt is the

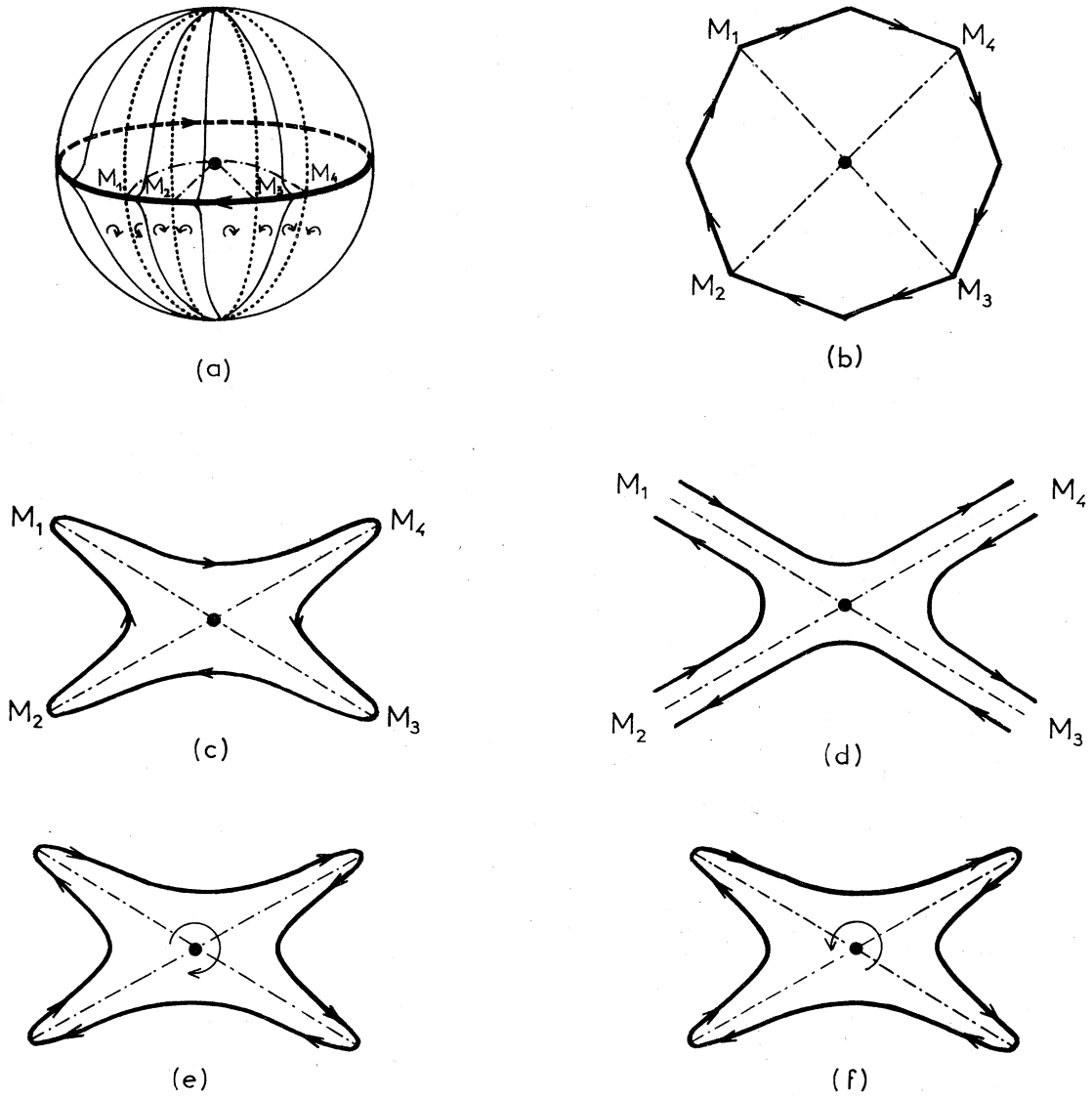

FIG. 2. (a) The topological representation of the meson-meson scattering amplitude $M_1M_2 \to M_3M_4$ by a quantum sphere covered by eight triangles and by a classical plane on which is embedded the corresponding Landau graph. The intersection of the classical and quantum surfaces is an oriented belt (the equatorial circle divided into eight segments). (b)–(d) Alternative representations of the classical surface. (e) Ortho and (f) para oriented classical surfaces. (g) Connected sums of spheres leading to a sphere. (h) Connected sums of cross-shaped classical surfaces leading to a cross-shaped classical surface.

intersection of the equatorial plane with the sphere: It is the equatorial circle passing through all trivial vertices and is divided into eight segments; these segments are delimited by the quark or antiquark triangles residing on the quantum sphere. The belt naturally acquires a well defined orientation, as a consequence of the patchwise orientation of the quantum surface. For example, if the segment of the belt delimited by a topological quark is oriented towards the trivial vertex, then the orientation of the contiguous topological antiquark is away from the corresponding trivial vertex. The belt thus acquires the continuous orientation shown in Fig. 2(a).

An alternative representation of the classical surface as an octagon is shown in Fig. 2(b). By continuous deformation of the octagon of Fig. 2(b) one obtains the cross shape shown in Fig. 2(c).

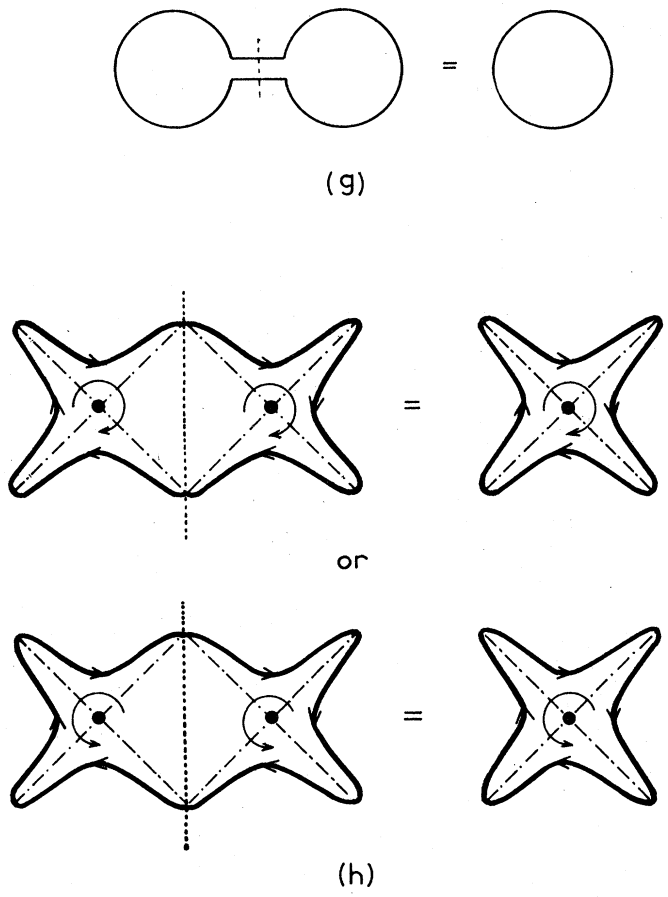

FIG. 2 (*Continued*.)

By opening the boundary at the points $M_1, \ldots, M_4$ one obtains a graph similar to the familiar Harari-Rosner duality diagram [Fig. 2(d)] which, however, as seen from Fig. 2(d), is supplemented with the corresponding Landau graph.

One can, of course, orient also the interior of the classical surface. This orientation can be in agreement ["ortho" orientation—Fig. 2(e)] or in disagreement ["para" orientation—Fig. 2(f)] with the orientation of the boundary. It is precisely this two-valued topological degree of freedom which allowed Stapp[5] to include the spin of the quark in the DTU theory.

One important feature of the zero-entropy level can now be visually stressed: The zero-entropy quantum and classical surfaces are self-reproducing under the connected sum (unitarity product) operation [Figs. 2(g) and 2(h)]. This is a graphical illustration of the previous statement that the nonlinearity of the bootstrap problem is concentrated at the zero-entropy level of the topological expansion. Of course, at the zero-entropy level, only ortho-ortho or para-para transitions are allowed on the classical surface [Fig. 2(h)]. In all other cases the entropy index increases due to the appearance of transition lines between ortho and para patches.

Examples of topological representations of more complicated amplitudes involving baryons will be given in Sec. IV.

III. THE SUPERSYMMETRY PROPERTY OF THE TOPOLOGICAL AMPLITUDES RELATING BOSONS TO FERMIONS

As was already stated in Sec. II, in the theory of Ref. 6 the spectrum of hadrons consists only of ordinary mesons, ordinary baryons, and baryonia. The four types of zero-entropy three-particle topological amplitudes ("coupling constants") are shown in Figs. 3(a)–3(d) and the six types of zero-entropy four-particle amplitudes are shown in Fig. 4.

We shall now show that the zero-entropy bootstrap leads naturally to a topological supersymmetric solution at this level of the topological expansion, in which the three-particle topological amplitudes of Fig. 3 are related to each other.

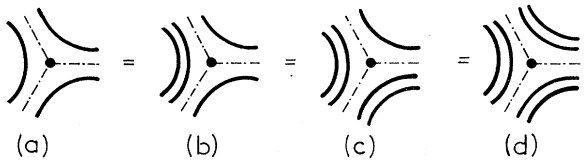

FIG. 3. The supersymmetry property for the four possible types of zero-entropy three-particle amplitudes, as seen on the classical surface. The quark-spin line directions are not indicated. The dashed-dotted lines represent Landau arcs.

We will use Stapp's M-function formalism.[5]

An M function is an analytic function of the particle four-momenta characterizing a given process, apart from isolated singularities described by the Landau graphical rules; it also has a well-defined crossing-principle property. It is not immediately equal to an S-matrix connected part but is related thereto by an explicit momentum-dependent spin-index transformation. Finally it depends on particle spin indices α_k which transform independently of the values of the momenta in changes of Lorentz frames of reference.

For a topological M function, each α_k is a collection of two-valued indices belonging to $(0, \frac{1}{2})$ or $(\frac{1}{2}, 0)$ spinor representations of the Lorentz group; a single such index is attached to each peripheral triangle of the corresponding particle disc. At the zero-entropy level the spin dependence then simply reduces to a product of Kronecker δ's (see Appendix D of the last paper of Ref. 6), one for each Harari-Rosner (HR) line joining two mated peripheral triangles (i.e., triangles which share all their vertices). One may then associate a single spin index to each HR line. (One can also note [see, e.g., Fig. 2(a)] that, even if, strictly speaking, flavor resides on the quantum surface, one can still make a one-to-one correspondence between the peripheral triangles carrying flavor and the corresponding HR line, lying on the belt. One may therefore also associate a single flavor index to each HR line.) The momentum dependence of a topological M function resides in a *separate* factor F.

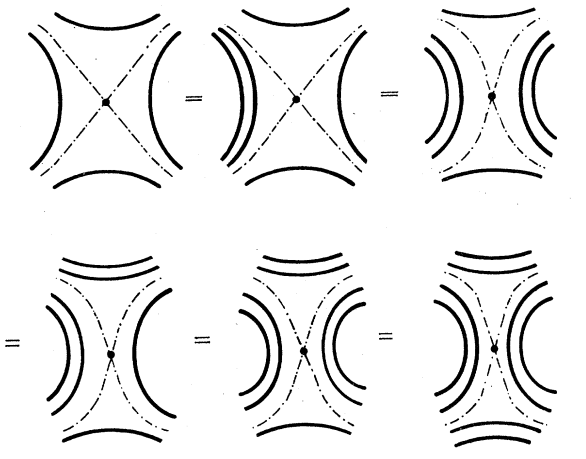

FIG. 4. The supersymmetry property for the six possible zero-entropy amplitudes, as seen on the classical surface. As in Fig. 3, the quark-spin line directions are not indicated.

The spin dependence of the M functions has the essential property of *transitivity* (self-reproducing) in zero-entropy connected sums.

Let us begin by considering an imaginary world in which the only particles are $q\bar{q}$ mesons (M_2). Its momentum-space dynamics would be represented by Fig. 5, where u, v, w are spin-flavor labels associated with the HR "quark" (q) lines and where it is understood that the left-hand side is merely shorthand notation for all possible total sums of "fishnet" graphs of the type shown in Fig. 6. We must consider all possible u, v and sum over all possible w. Because of our spin-momentum factorization the resulting equations are clearly symmetric with respect to the values of the u, v, w labels. The usual (label-value-degenerate) solution of this bootstrap, if it exists, then gives all possible M_2 mass ratios and couplings $\hat{g}$. The latter are given by conditions of the form $\hat{g}^2 N_{\bar{q}} \sim 1$, where $N_{\bar{q}}$ is a spin-flavor multiplicity factor arising from the summation over w. We have used the spin-momentum factorization result that each of the terms in the sum of Fig. 5 gives the same contribution in this case.

Let us next turn to a realistic zero-entropy world which also includes $qqq(B_3)$ and $\bar{q}\bar{q}qq(M_4)$ states. We must now replace Fig. 5 by Fig. 7, where we have also introduced spin-flavor labels u', v', w' associated with the (qq) "diquark" double lines. Because of our spin-momentum factorization, however, we see that, given the solution of the previous paragraph (to the equations represented by Fig. 5), we immediately have a solution to the bootstrap of Fig. 7 in which the masses of corresponding M_2, B_3, and M_4 states are equal. Such a solution would satisfy label-value-degenerate equations which are identical to formally re-

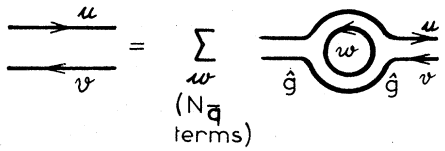

FIG. 5. Bootstrap dynamics in a zero-entropy world containing only M_2 mesons.

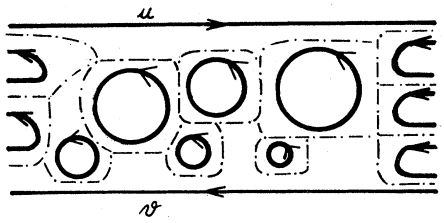

FIG. 6. A given fishnet graph.

placing each (qq) by $\bar{q}$ and collapsing Fig. 7 into Fig. 5, but with extended u, v, w labels and with $N_{\bar{q}} \to N_{\bar{q}} + N_{qq}$. Indeed, since each of the terms in the sum over w of this modified Fig. 5 gives the same contribution in this case, the corresponding coupled integral equations can be reduced exactly to ones satisfied by our solution of the original Fig. 5, making only trivial numerical rescalings of the amplitudes involved. In particular, we obtain exactly the same M_2 Regge trajectories in the two cases (at least if we use the same energy scale to normalize our masses) whereas $\hat{g}^2 \to g^2 = \hat{g}^2 N_{\bar{q}}/(N_{\bar{q}} + N_{qq})$ where g $(= g_{M_2 M_2 M_2} = g_{M_2 B_3 \bar{B}_3} = \cdots)$ is then any given coupling.

Thus, given our solution of the bootstrap equations for the original imaginary (M_2 only) zero-entropy world of Fig. 5 we also trivially have a supersymmetric solution for the expanded world of Fig. 7. If we make the usual bootstrap assumption that our zero-entropy bootstrap (Fig. 7) must have a unique solution, this supersymmetric solution is also the only solution at this level; in particular, we then obtain the equalities of Figs. 3 and 4.

It is important to note that the trivial numerical rescaling $N_{\bar{q}} \to N_{\bar{q}} + N_{qq}$ is in fact crucial from the physical point of view. Owing to the fact that each closed quark loop carries a (-1) factor,[5] the hadron spectrum cannot consist only of ordinary mesons: A consistent world has to contain also at least baryons and baryonia. Here we considered that the hadron spectrum terminates at the baryonium level. However, it can be easily verified that our results are valid even when one assumes that other multiquark hadrons are present.

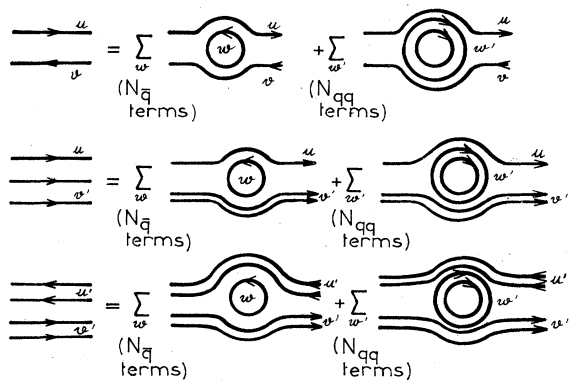

FIG. 7. Expanded bootstrap dynamics in a zero-entropy world containing M_2, B_3, and M_4 hadrons.

The supersymmetry property can be intuitively stated by introducing the notion of "active" and "spectator" quarks. The active quarks are the quarks which correspond to quark lines on the classical surface which are immediate neighbors of a Landau arc (see Fig. 3), while the spectator quarks are those quarks which correspond to quark lines on the classical surface which are not immediate neighbors of a Landau arc. The couplings (b), (c), and (d) (see Fig. 3) are obtained from the coupling (a) (which involves only active quarks) by adding each time a new spectator quark. Roughly speaking, topological supersymmetry amounts to the statement that adding spectator quarks at zero entropy changes nothing. The same statement is true for the topological amplitudes of Fig. 4. The addition of spectator quarks changes, of course, the spin description (via the quark lines of the classical surface) but leaves unchanged the dynamics described by Landau graphs. Rigorously speaking, the notion of active and spectator quarks requires "thickened" Landau graphs th(L) [see Appendix B of the last paper of Ref. 6 for a precise topological definition of th(L)], together with the association of a cyclic order on the quantum surface with the order of quarks within a diquark (i.e., a pair consisting of an active and a spectator quark).

The existence of a topological-supersymmetric solution for the M functions does not immediately imply supersymmetry for S-matrix connected parts. The two are related by explicit momentum-dependent spin-index transformations which may be different for different amplitudes. In particular, when we make the replacement $\bar{q} \to (qq)$ we generally obtain a difference from the fact that $\bar{q}$ propagates spin in the sense reverse to (qq) in a hadron. As long as the particle momentum is the same at the two ends of a quark line ("forward scattering") this direction reversal makes no difference, however. In addition, the amplitude structure arising from our momentum-dependent spin-index transformations simplifies considerably at high energies, making it possible to essentially ignore spin complications (in the usual sense) and directly apply supersymmetry to a comparison of two forward amplitudes at high energies.

One might note that the topological supersymmetry is a property peculiar to the zero-entropy level of the topological expansion. Supersymmetry must be broken by higher orders of the topological

expansion.

The supersymmetry property is not explicitly stated in the theory of Ref. 6. However, as we just showed, it can in fact be derived from this theory.

IV. TOPOLOGICAL SUPERSYMMETRIC STRUCTURE OF HADRON CROSS SECTIONS

A. Topological structure of hadron cross sections

Let us start with hadron-nucleon total cross sections. Through the optical theorem, they are proportional to the imaginary parts of forward elastic amplitudes and we know that such hadron amplitudes have a topological representation via the quantum and classical surfaces.

It is well known that the channels having the quantum numbers of the Pomeron are strongly affected by the higher orders of the topological expansion.[1] Since we want to test the zeroth order of the topological expansion, we choose to deal with the amplitudes which are antisymmetric under crossing, i.e., we study the *differences* of the antihadron-nucleon and hadron-nucleon total cross sections

$$\Delta\sigma_{HN}(s) \equiv \sigma_{\bar{H}N}(s) - \sigma_{HN}(s) = \frac{1}{2m_N p_L} \operatorname{Im} F^{(-)}_{HN\to HN}(s, t=0), \tag{1}$$

where m_N is the mass of the nucleon.

Let us now study the implications of the DTU theory for the amplitudes which come into Eq. (1).

At zero entropy, the discs which represent the initial particles on the one hand and the final particles on the other are contracted in all possible ways in order to build channel discs. Then, by unitarity, the amplitudes are obtained by gluing together these channel discs so as to cover the quantum sphere. It can happen that different gluing operations lead to the *same* pair of quantum and classical surfaces. This topological equivalence leads to a well-defined topological structure for $\Delta\sigma$. For example, it can be seen from Fig. 8 that in the $p\bar{p}$ s channel there are five possible ways of gluing together a proton p and an antiproton $\bar{p}$ so that we obtain a $p\bar{p}$ channel disc of the baryonium type. Then there are five connections of one channel disc with itself [the amplitude in Eq. (1) is elastic] which lead to the *same* quantum and classical surfaces. (Here u-d symmetry is naturally assumed.) Each baryonium channel disc is dual to a channel disc of the ordinary meson type in the t channel.

One can obviously also form $p\bar{p}$ s channel discs of the ordinary meson type, which are dual to t-channel baryonium-type discs. But we established above that, for the case of baryonium channel discs, one obtains five identical contributions. The fact that the baryonium is now in the t channel is irrelevant, the s and t channels being identical in $p\bar{p}\to p\bar{p}$ scattering.

It is clear that no channel disc can be formed in pp scattering (the gluing is performed only via quark-antiquark pairs). The disc contribution to σ_{pp} is therefore zero.

From the above considerations, we finally obtain

$$\Delta\sigma_{p\bar{p}} = 5\sigma^{(M_4)}_{M_2} + 5\sigma^{(M_2)}_{M_4}, \tag{2}$$

where σ_{M_2} and σ_{M_4} correspond to quantum spheres whose t-channel discs are of the ordinary meson (M_2) and baryonium (M_4) types; the upper index of σ refers to the nature of the s-channel discs.

In a similar way, we obtain, for the first generation of quarks (u and d), that there are (always in the s channel) four M_4 contributions and four M_2 contributions in the case of $\bar{p}n$ scattering, no contribution for pn scattering, two baryon (B_3) contributions for $\pi^- p$, one B_3 contribution for $\pi^+ p$ scattering, one B_3 contribution for $\pi^- n$ and two B_3 contributions for $\pi^+ n$ scattering. We therefore obtain

$$\Delta\sigma_{pn} = 4\sigma^{(M_4)}_{M_2} + 4\sigma^{(M_2)}_{M_4}. \tag{3}$$

and

$$\Delta\sigma_{\pi p} = -\Delta\sigma_{\pi n} = \sigma^{(B_3)}_{M_2}. \tag{4}$$

From Eqs. (2) and (3) we obtain the following relation between $\Delta\sigma_{p\bar{p}}$ and $\Delta\sigma_{pn}$:

$$\tfrac{1}{5}\Delta\sigma_{p\bar{p}} = \tfrac{1}{4}\Delta\sigma_{pn}. \tag{5}$$

It is important to note the *absence* of the term σ_{M_4} in $\Delta\sigma_{\pi p}$ and $\Delta\sigma_{\pi n}$ which is a consequence of one of the most remarkable manifestations of the topological selection rules[10]: the noncommunication on the sphere between baryonium and ordinary meson channels.

It should also be noted that the superposition of zero-entropy topological amplitudes M within the topological expansion

$$M_{fi} = \sum_{\gamma} M^{\gamma}_{fi} \tag{6}$$

(where γ is the topological complexity index, f the final state, and i the initial state) carries no coefficients that depend on f and i. For example, we do not insert factors like $1/\sqrt{6}$ for each baryon. The rule (6) can be justified on the basis of unitarity and cluster decomposition.[11]

By means of the Mueller generalized optical theorem, we can make the same topological analysis in the case of the inclusive reactions $\pi^{\pm} p \to \pi^{\pm} X$ and $p^{\pm} p \to \pi^{\pm} X$ in the fragmentation region of the proton target, where there exists a coherent set of

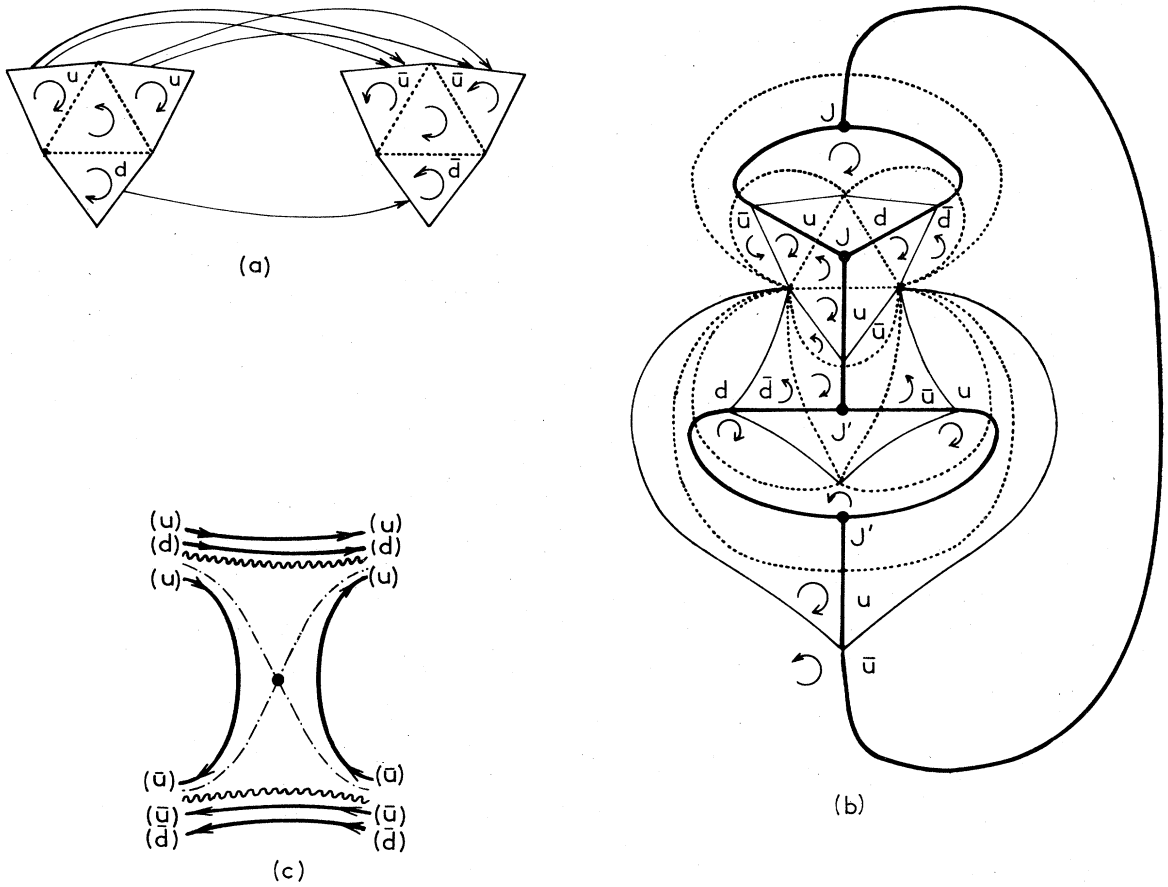

FIG. 8. (a) The five possible ways of obtaining the $p\bar{p}$ s-channel baryonium disc by the contraction of a quark-antiquark pair. (b) One of the corresponding $p\bar{p} \to p\bar{p}$ quantum spheres. The dotted edges delimit the core triangles, while the solid edges delimit the peripheral triangles. The heavy solid curve is the belt—see Ref. 6. (c) The $p\bar{p} \to p\bar{p}$ classical surface corresponding to the "belt" of (b). The heavy solid lines represent quark-spin lines, the dashed-dotted lines represent Landau arcs, while the wiggly lines represent junction lines. The flavor indices, which actually reside on the quantum sphere, are indicated merely to guide the eye.

data. From a topological point of view, we will consider the pion to belong to the fragmentation region of the proton when the pion disc shares at least one quark triangle with the proton disc. For example, Fig. 9 shows a possible configuration which is allowed at the lowest entropy level whereas Fig. 10 shows a configuration which is forbidden at the same level due to an increase of the topological complexity index attached to the classical surface: It can be seen from Fig. 10 that a Landau line has to cross a junction line. After having counted all possibilities, we find

$$\Delta\sigma_{\pi p \to \pi^- X} = \sigma_{M_2}^{(B_3)'} \tag{7}$$

$$\Delta\sigma_{\pi p \to \pi^+ X} = -2\sigma_{M_2}^{(B_3)'}, \tag{8}$$

$$\Delta\sigma_{pp \to \pi^- X} = 2\sigma_{M_2}^{(M_4)'} + \sigma_{M_4}^{(M_2)'}, \tag{9}$$

$$\Delta\sigma_{pp \to \pi^+ X} = 2\sigma_{M_2}^{(M_4)'} + 4\sigma_{M_4}^{(M_2)'}, \tag{10}$$

where σ'_{M_2} and σ'_{M_4} have the same meaning as σ_{M_2} and σ_{M_4}. From Eqs. (7) and (8) we obtain the following interesting relation:

$$\Delta\sigma_{\pi p \to \pi^+ X} = -2\Delta\sigma_{\pi p \to \pi^- X}. \tag{11}$$

We can make a similar analysis of the cross sections involving s quarks. However, a clear analysis of these cross sections involves an understanding of the problem of quark generations which is, of course, not yet solved. We are confronted by the following alternative: Either (1) there is a SU(N) flavor symmetry at the lowest-entropy level, which has subsequently to be broken by a mechanism as yet unknown or (2) the quarks which do not belong to the first generation are not associated with the peripheral triangles, but, rather, with more complicated topological forms (e.g., spheres or tori), so that there is a "break-

ing" from the beginning: Only the u and d quarks then appear at the lowest-entropy level.

We can make certain predictions which do not depend on which of the two aforementioned cases is assumed. Namely, we treat s as an index with an unspecified topological form and we assume once again that the hadron interaction proceeds via the minimum-possible-entropy contribution. We then obtain the following relations:

$$\tfrac{1}{2}\Delta\sigma_{Kp}=\Delta\sigma_{Kn}=\sigma_{M_2}^{(B_3)''}, \tag{12}$$

$$\Delta\sigma_{kp\to\pi^- X}=\sigma_{M_2}^{(B_3)'''}, \tag{13}$$

$$\Delta\sigma_{kp\to\pi^+ X}=0. \tag{14}$$

An important feature of our analysis has to be stressed here. In the case of the total cross sections, the relations (2)–(5) and (12) can also be obtained in models which combine the usual Harari-Rosner duality diagrams (where the flavors are associated with the classical surface) with the additive quark model.[12] Of course, good empirical relations can sometimes be obtained for the wrong reasons. In any case, the above-mentioned parallelism is generally not valid. Because of our richer topological content, the higher-order corrections are different from those of the previous models. Even more important is the fact that in the case of the inclusive cross sections the information coming from the lowest order of the theory of Ref. 6 is different from that obtained from the previous models. The difference comes essentially from the explicit consideration of the Landau graphs on the classical surface. For example, the graph shown in Fig. 10(c) would be considered, in the absence of the Landau graph, as a perfectly planar, allowed diagram. The topological mechanism for the suppression of the graphs involving intersections between Landau lines and junction lines was previously ignored. Clearly then the conclusions based on the old formalism of Harari-Rosner duality diagrams are not always equivalent to our present conclusions. For example, if we ignore intersections between a Landau line and a junction line, we obtain a nonvanishing value for the difference between the cross sections for $K^- p\to\pi^+ X$ and $K^+ p\to\pi^+ X$.

The overall agreement of our relations with the experimental data (see Sec. V) is an *a posteriori* argument for the necessity of this topological graph-suppression mechanism.

B. Relations between hadron cross sections based on the topological supersymmetry property

Topological supersymmetry has important consequences at the practical level. For example, the second equality belonging to the series of relations shown symbolically in Fig. 4 implies that

$$\sigma_{M_2}^{(B_3)}=\sigma_{M_2}^{(M_4)}\equiv\sigma. \tag{15}$$

We therefore find, from Eqs. (2), (4), and (15), that

$$\tfrac{1}{5}\Delta\sigma_{pp}-\Delta\sigma_{\pi p}=\sigma_{M_4}^{(M_2)}>0. \tag{16}$$

The supersymmetry property also implies that

$$\sigma_{M_2}^{(B_3)'}=\sigma_{M_2}^{(M_4)'}\equiv\sigma', \tag{17}$$

which, when combined with Eqs. (7)–(10), gives

$$\tfrac{1}{2}\Delta\sigma_{pp\to\pi^- X}-\Delta\sigma_{\pi p\to\pi^- X}=\tfrac{1}{2}\sigma_{M_4}^{(M_2)'}>0, \tag{18}$$

$$\Delta\sigma_{pp\to\pi^- X}+\Delta\sigma_{\pi p\to\pi^+ X}=\sigma_{M_4}^{(M_2)'}>0, \tag{19}$$

$$\tfrac{1}{2}\Delta\sigma_{pp\to\pi^+ X}-\Delta\sigma_{\pi p\to\pi^- X}=2\sigma_{M_4}^{(M_2)'}>0, \tag{20}$$

$$\Delta\sigma_{pp\to\pi^+ X}+\Delta\sigma_{\pi p\to\pi^+ X}=4\sigma_{M_4}^{(M_2)'}>0. \tag{21}$$

Of course, for sufficiently high energies, the baryonium contribution is expected to be negligible:

$$\sigma_{M_4}^{(M_2)}\simeq 0, \quad \sigma_{M_4}^{(M_2)'}\simeq 0. \tag{22}$$

In this case, Eq. (16) becomes the well-known Freund relation[13]

$$\tfrac{1}{5}\Delta\sigma_{pp}=\Delta\sigma_{\pi p}, \tag{23}$$

and one also obtains the remarkable relations

$$\tfrac{1}{2}\Delta\sigma_{pp\to\pi^- X}=\Delta\sigma_{\pi p\to\pi^- X}, \tag{24}$$

$$\Delta\sigma_{pp\to\pi^+ X}=-\Delta\sigma_{\pi p\to\pi^+ X}, \tag{25}$$

the differences of cross sections involving a proton beam being approximately equal at high energies:

$$\Delta\sigma_{pp\to\pi^- X}=\Delta\sigma_{pp\to\pi^+ X} \tag{26}$$

as can be seen from Eqs. (9), (10), and (22).

In the next section we will see that the equations obtained as a consequence of the supersymmetry property are in general agreement with the experimental data.

V. COMPARISON WITH THE EXPERIMENTAL DATA

We will use the data for total cross sections which can be found in Ref. 14 and the data for inclusive cross sections given in Ref. 15.

Let us begin by making a general remark: Contrary to what we might expect superficially, the data for total cross sections are sufficiently precise to test our relations in an unambiguous manner. It is commonly believed that cross-section differences are subject to errors which are comparable with the data themselves (and this statement is, of course, true for the raw data). However, if we *first* make a best interpolation of total cross sections (and this is effectively what we did

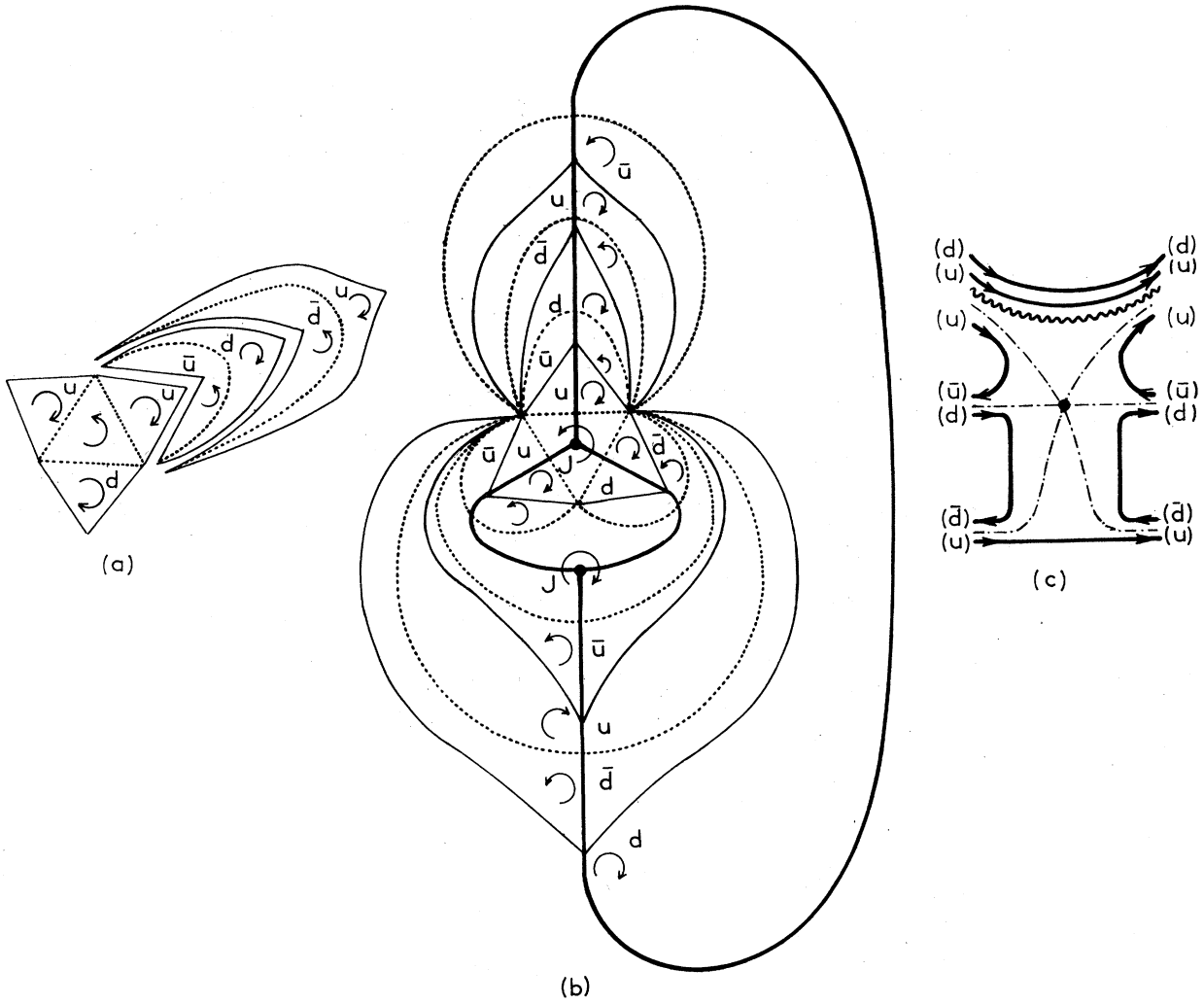

FIG. 9. (a) The building of a channel disc for $\pi^+ p \to \pi^+ X$ in the fragmentation region of the proton. (b) A quantum sphere and (c) a classical surface corresponding to the reaction $\pi^+ p \to \pi^+ X$. The notation is the same as in Fig. 8.

for data involving proton targets) and then compute the corresponding differences, we obtain rather small errors for $\Delta\sigma$, simply because the data combining both low and high energies are in fact very accurate. The particular parametrization used to interpolate the data is obviously not very interesting in itself (and we will not describe it here), the only important thing being the use of a best interpolation in order to describe in an accurate manner the general trend of the data.

The situation for the total cross-section data involving a neutron target is slightly different. The data are subject to bigger errors, due to the fact that a theoretical model (the Glauber model) is used to extract the neutron data. For this reason we will use, in this case, the raw data directly. However, their precision will be sufficient to clearly test our relations.

Finally, the inclusive data are the most ambiguous from the point of view of testing our relations. This is not essentially connected with the actual precision of the measurements themselves, but rather with the fact that the experimental numbers are obtained as the result of an integration in somewhat different ranges of rapidity by different experimental groups.[15,16] However, since the experimental results are practically the same, this does not affect our analysis. In any case, here too we will use raw data, which exhibit in a sufficiently clear manner the general trends existing in the data.

In testing our relations we will discuss sepa-

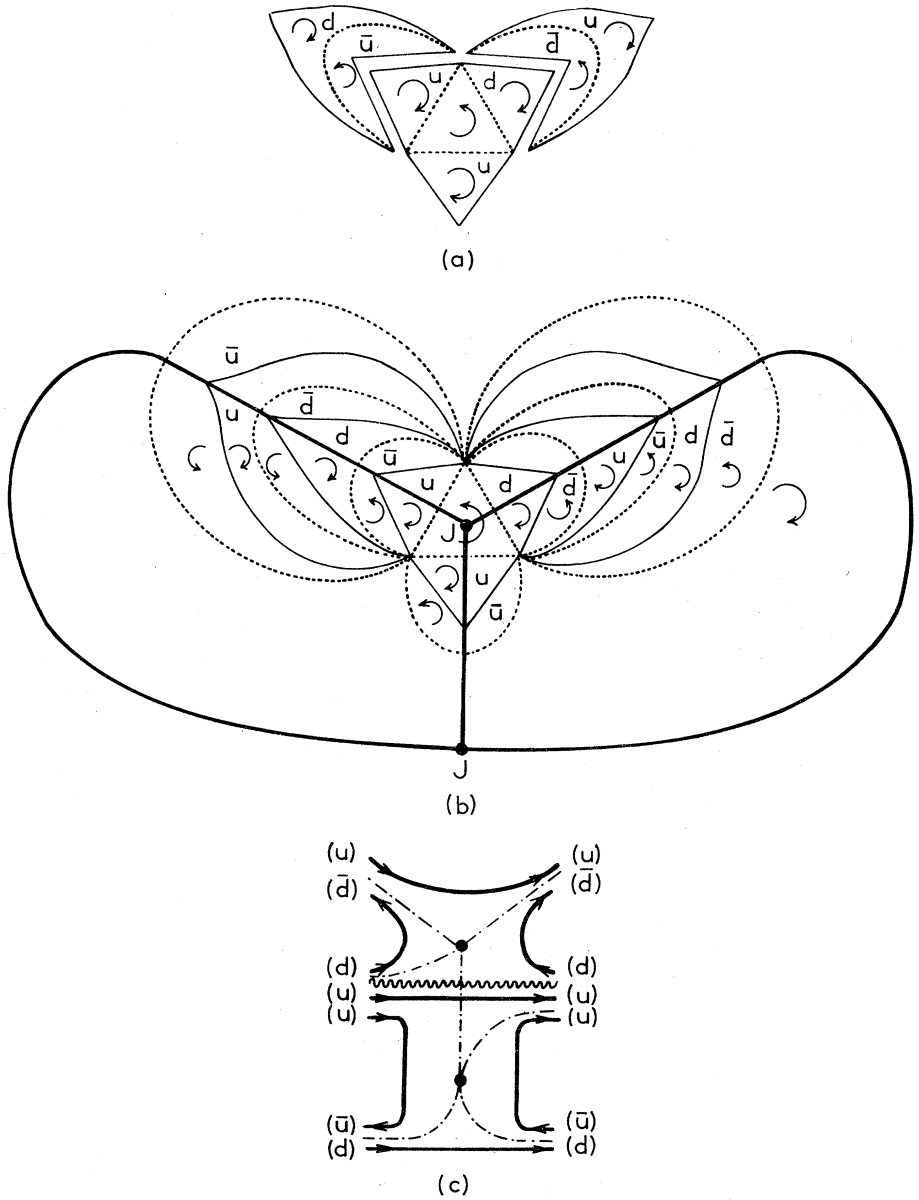

FIG. 10. A forbidden contribution at the lowest-entropy level in $\pi^- p \to \pi^- X$. One may note the intersection between the Landau line and the junction line in (c).

rately the relations which are obtained without the explicit use of the supersymmetry property and those which are based upon this property.

A. Relations between hadron cross sections which are independent of the topological supersymmetry property

The relation (5) between $\Delta\sigma_{pp}$ and $\Delta\sigma_{pn}$ appears to be in nice agreement with the experimental data (see Fig. 11).

The relation (12) between $\Delta\sigma_{Kp}$ and $\Delta\sigma_{Kn}$ is also in nice agreement with the experimental data (see Fig. 12).

Equation (11) correctly predicts the opposite sign of $\Delta\sigma_{\pi p \to \pi^+ X}$ relative to $\Delta\sigma_{\pi p \to \pi^- X}$ (see Fig. 13). However, their ratio (-2) is not in agreement with the experimental ratio $\simeq -1$. As can be readily checked, the origin of the coefficients 1 and -2 in Eqs. (7) and (8) lies simply in the fact that the proton has two times as many u quarks as d quarks. This naive quark-counting rule was shown in the past to lead to realistic predictions for other sets of data.[17] Of course, we saw that such naive

quark-counting rules are not valid in general, the results being modified by the suppressions arising from the intersection of Landau lines with junction lines. However, in particular cases, like the one just discussed, the naive results remain unchanged.

It is also interesting to notice that an overall Regge-pole fit of inclusive data[8] requires a value -2 for the above-mentioned ratio. It therefore seems to us that a careful reanalysis of the experimental data for $\pi^{\pm}$ inclusive production would be worthwhile. New experiments on these processes would also be welcome.

The approximate equality of $\Delta\sigma_{pp\to\pi^- X}$ and $\Delta\sigma_{pp\to\pi^+ X}$ at high energies [Eq. (26)] is satisfied by the data in the range $15 \lesssim p_L \lesssim 150$ GeV/c (see Fig. 13).

Finally, the vanishing of $\Delta\sigma_{Kp\to\pi^+ X}$ predicted by Eq. (14) is also compatible with the data for $8 \lesssim p_L \lesssim 150$ GeV/c (Fig. 14). It is interesting to note that if one ignores the intersections between Landau lines and junction lines (glitches), one obtains, in particular, a nonvanishing $\Delta\sigma_{Kp\to\pi^+ X}$ in disagreement with the data. This result shows once again the importance of the topological selection rules originating from the classical surface.[10] As we stressed in Sec. IV A existing quark models ignore this topological suppression of graphs due to glitches and they therefore lack, in our opinion, an important piece of dynamical information.

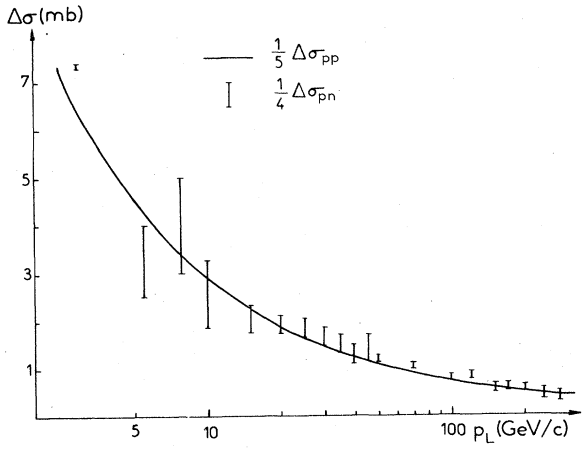

FIG. 11. The experimental verification of Eq. (5) (see text). The solid curve represents the best fit of $\Delta\sigma_{p\bar{p}}$ obtained via the best fit of the $p\bar{p}$ and pp total cross sections themselves. This curve is subject to an overall ~5% error (not shown in the figure). The bars represent raw data $\Delta\sigma_{pn}$ data.

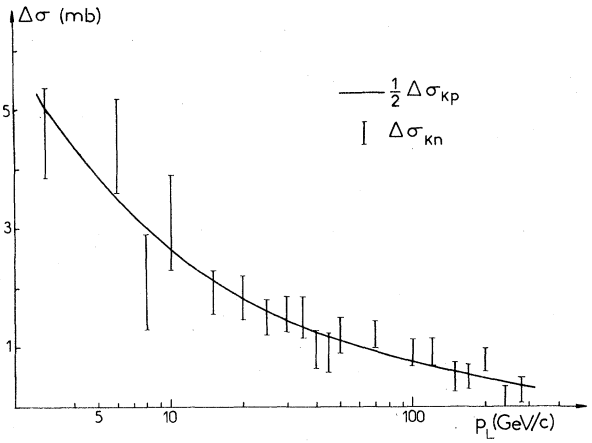

FIG. 12. The experimental verification of Eq. (12) (see text). The solid curve is affected by an overall ~10% error.

B. Relations between hadron cross sections which are based on the topological supersymmetry property

Let us now turn to the relations (16) and (18)–(21) which were obtained using the supersymmetry property.

The relation (16) is supported in a spectacular manner by the experimental data (Fig. 15). The nonvanishing of the difference of cross sections involved in Eq. (16) can be regarded as one of the most convincing phenomenological proofs of the existence of baryonium (in the absence of baryonium, the χ^2 corresponding to the curve in Fig. 15 is $\chi^2/\text{point} \simeq 100$ in the region $4 \lesssim p_L \lesssim 50$ GeV/c).

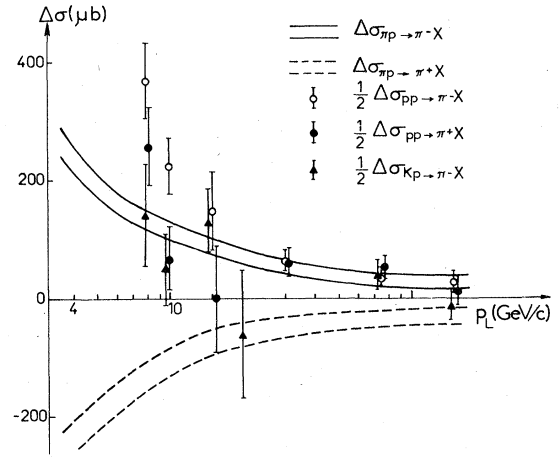

FIG. 13. The experimental verification of Eqs. (11), (18)–(21), and (24)–(26) (see text).

This conclusion is in agreement with the somewhat less constrained analysis of Gavai and Roy.[18,19] It is the presence of baryonium which is responsible for the violation of the Freund relation (23) below $p_L \lesssim 50$ GeV/c. The contribution of baryonium obviously corresponds to a Regge-pole behavior (Fig. 16). The baryonium intercept lies in the well-known range[18,20] $-1 \lesssim \alpha_{M_4}(0) \lesssim 0$.

The relations (18)–(21), (24), and (25) are more difficult to test, owing to the lack of precise inclusive data at low energies and the possible problem connected with the inclusive production data which was mentioned above when we discussed Eq. (11). However, it is nevertheless important to note that the positive sign of the cross-section combinations (18)–(21) is in clean agreement with the data (see Fig. 13), pointing to a baryonium contribution. One may also note that the relations (24) and (26), which have to be valid at high energies, are in agreement with the data for $15 \lesssim p_L \lesssim 150$ GeV/c, while the relation (25) is not satisfied by the data. We find here a hint that the doubtful π-inclusive production data are probably the π^+ data.

Let us close with a note concerning SU(3) flavor symmetry. As can be seen from Fig. 17, $\frac{1}{2}\Delta\sigma_{Kp}$ approaches the common limit of $\Delta\sigma_{\pi p}$ and $\frac{1}{5}\Delta\sigma_{pp}$ after $p_L \simeq 30$ GeV/c, indicating [from Eqs. (4) and (12)] that

$$\sigma_{M_2}^{(B_3)''} \simeq \sigma_{M_2}^{(B_3)}. \tag{27}$$

The Johnson-Treiman relation[21]

$$\tfrac{1}{2}\Delta\sigma_{Kp} = \Delta\sigma_{\pi p} \tag{28}$$

is therefore approximately valid at high energies. Also, as can be seen from Fig. 13, $\Delta\sigma_{Kp\to\pi^- X}$ approaches $\Delta\sigma_{\pi p\to\pi^- X}$ for $p_L \gtrsim 8$ GeV/c, indicating [from Eqs. (7) and (13)] that

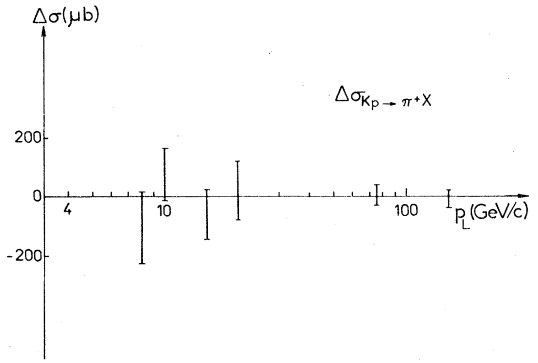

FIG. 14. The experimental verification of the vanishing of $\Delta\sigma_{Kp\to\pi^+X}$ predicted by Eq. (14).

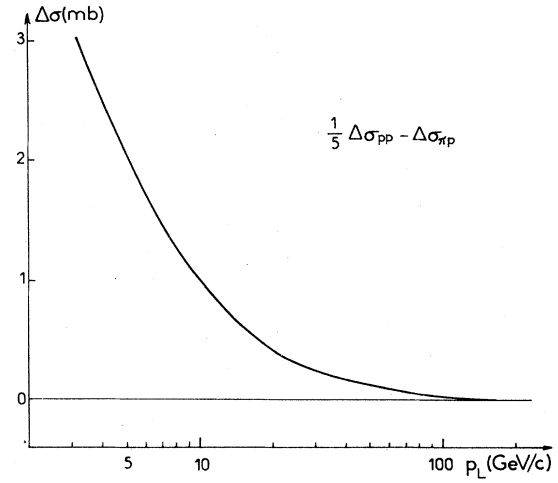

FIG. 15. The experimental verification of Eq. (16) (see text) as a hint for the existence of baryonium.

$$\sigma_{M_2}^{(B_3)''} \simeq \sigma_{M_2}^{(B_3)'}. \tag{29}$$

One can interpret these relations as being a manifestation of SU(3) flavor symmetry (at least for sufficiently high energies). However, the big nonzero difference between $\frac{1}{2}\Delta\sigma_{Kp}$ and $\Delta\sigma_{\pi p}$ at low and medium energies (see Fig. 17) also exhibits the existence of a big breaking of this symmetry. We therefore think that the simultaneous existence of (i) a big nonzero difference between $\frac{1}{2}\Delta\sigma_{Kp}$ and $\Delta\sigma_{\pi p}$ at low and medium energies and (ii) the near equality of $\frac{1}{2}\Delta\sigma_{Kp}$ and $\Delta\sigma_{Kn}$ for the entire range of energies seems to indicate that the second possibility mentioned in Sec. IV A concerning the problem of flavor generations is empirically favored. Of course, this is just a hint, not a demonstration. It is obvious that as long as masses are negligible, SU(3) flavor symmetry is effectively restored. In any case all our predictions discussed above are

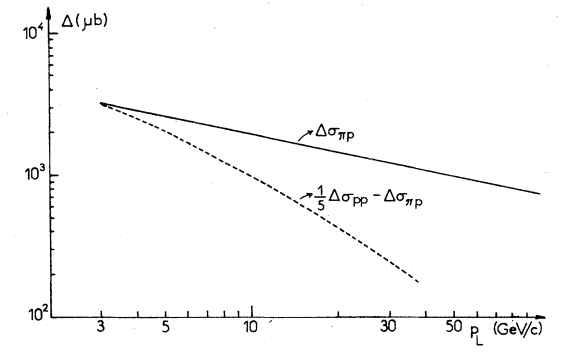

FIG. 16. The Regge-pole behavior of the baryonium contribution (dashed curve) compared with the familiar ρ-Regge-pole contribution (solid curve).

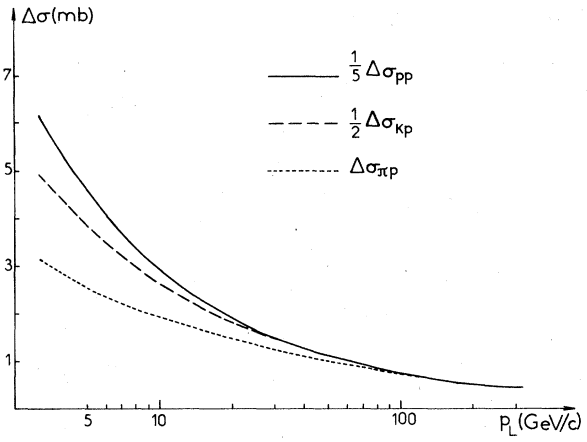

FIG. 17. The common limit of $\frac{1}{5}\Delta\sigma_{pp}$, $\frac{1}{2}\Delta\sigma_{Kp}$, and $\Delta\sigma_{\pi p}$ at high energies.

independent of the assumption of SU(3) flavor symmetry.

VI. CONSEQUENCES OF THE TOPOLOGICAL STRUCTURE OF HADRON CROSS SECTIONS ON REGGE COUPLINGS

Let us consider the leading Regge contributions to $\Delta\sigma$, namely ρ and ω, which are exchange-degenerate at the lowest entropy level,

$$\alpha_\rho = \alpha_\omega \equiv \alpha_R . \tag{30}$$

We will assume, as usual,[1] that ω is built up only out of u and d quarks.

We therefore obtain, from Eqs. (2)–(4), (7)–(10), (15), (17), and (22), with the obvious notation for Regge couplings,[8] the following system of equations at high energies:

$$\Delta\sigma_{pp} = 2[(\gamma_p^\rho)^2 + (\gamma_p^\omega)^2]s^{\alpha_R - 1} = 5\sigma , \tag{31}$$

$$\Delta\sigma_{pn} = 2(\gamma_p^\rho\gamma_n^\rho + \gamma_p^\omega\gamma_n^\omega)s^{\alpha_R - 1} = 4\sigma , \tag{32}$$

$$\Delta\sigma_{\pi p} = 2\gamma_p^\rho\gamma_\pi^\rho s^{\alpha_R - 1} = \sigma , \tag{33}$$

$$\Delta\sigma_{\pi n} = 2\gamma_n^\rho\gamma_\pi^\rho s^{\alpha_R - 1} = -\sigma , \tag{34}$$

$$\Delta\sigma_{pp\to\pi^- X} = 2(\gamma_p^\rho F_{p\pi^-}^\rho + \gamma_p^\omega F_{p\pi^-}^\omega)s^{\alpha_R - 1} = 2\sigma' , \tag{35}$$

$$\Delta\sigma_{pp\to\pi^+ X} = 2(\gamma_p^\rho F_{p\pi^+}^\rho + \gamma_p^\omega F_{p\pi^+}^\omega)s^{\alpha_R - 1} = 2\sigma' , \tag{36}$$

$$\Delta\sigma_{\pi p\to\pi^- X} = 2\gamma_\pi^\rho F_{p\pi^-}^\rho s^{\alpha_R - 1} = \sigma' , \tag{37}$$

$$\Delta\sigma_{\pi p\to\pi^+ X} = 2\gamma_\pi^\rho F_{p\pi^+}^\rho s^{\alpha_R - 1} = -2\sigma' . \tag{38}$$

From Eqs. (33) and (34) we obtain

$$\gamma_p^\rho = -\gamma_n^\rho \tag{39}$$

which, together with the assumed relation

$$\gamma_p^\omega = \gamma_n^\omega , \tag{40}$$

is simply a statement of the charge independence of strong interactions. From Eqs. (31), (32), (39), and (40) we then obtain

$$\gamma_p^\rho = \tfrac{1}{2}\gamma_\pi^\rho . \tag{42}$$

Equations (41) and (42) are nothing other than manifestations of the celebrated ρ universality and ω universality properties, which are known to be not too badly violated when compared with experiment.[8] From Eqs. (35), (37), (41), and (42) we obtain

$$F_{p\pi^-}^\rho = F_{p\pi^-}^\omega , \tag{43}$$

and from Eqs. (36), (38), (41), and (42) we obtain

$$F_{p\pi^+}^\rho = -F_{p\pi^+}^\omega . \tag{44}$$

Of course, we also have, from Eqs. (37) and (38),

$$F_{p\pi^+}^\rho = -2F_{p\pi^-}^\rho . \tag{45}$$

The ω couplings satisfy a relation similar to (45) which follows from Eqs. (43)–(45):

$$F_{p\pi^+}^\omega = 2F_{p\pi^-}^\omega . \tag{46}$$

All these results are obviously independent of the assumption of SU(3) flavor symmetry, but some of them are dependent on the assumption of our supersymmetry property.

It would be interesting now to take into account the cross sections involving K mesons and to *assume* SU(3) flavor symmetry. From Eqs. (12)–(15), (17), (27), and (29), we then obtain

$$\Delta\sigma_{Kp} = 2(\gamma_p^\rho\gamma_K^\rho + \gamma_p^\omega\gamma_K^\omega)s^{\alpha_R - 1} = 2\sigma , \tag{47}$$

$$\Delta\sigma_{Kn} = 2(\gamma_n^\rho\gamma_K^\rho + \gamma_n^\omega\gamma_K^\omega)s^{\alpha_R - 1} = \sigma , \tag{48}$$

$$\Delta\sigma_{Kp\to\pi^- X} = 2(\gamma_K^\rho F_{p\pi^-}^\rho + \gamma_K^\omega F_{p\pi^-}^\omega)s^{\alpha_R - 1} = \sigma' , \tag{49}$$

$$\Delta\sigma_{Kp\to\pi^+ X} = 2(\gamma_K^\rho F_{p\pi^+}^\rho + \gamma_K^\omega F_{p\pi^+}^\omega)s^{\alpha_R - 1} = 0 . \tag{50}$$

It is easy to see that Eqs. (47), (48), and (39)–(41) imply

$$\gamma_K^\rho = \gamma_K^\omega , \tag{51}$$

which is an exchange-degeneracy relation, while Eqs. (33), (41), (42), (47), and (51) imply

$$\gamma_K^\rho = \gamma_p^\rho , \tag{52}$$

which is again a manifestation of the ρ universality property.

It is amusing to note that because $\Delta\sigma_{pp\to\pi^\pm X}$ are equal to $2\sigma'$ [Eqs. (35) and (36)], $\Delta\sigma_{\pi p\to\pi^- X}$ and $\Delta\sigma_{Kp\to\pi^- X}$ are equal to σ' [Eqs. (37) and (49)], $\Delta\sigma_{\pi p\to\pi^+ X}$ is equal to $-2\sigma'$ [Eq. (38)] and $\Delta\sigma_{Kp\to\pi^+ X}$ is equal to 0 [Eq. (50)], one trivially gets the relation

$$\Delta\sigma_{pp\to\pi^\pm X} = 3\Delta\sigma_{Kp\to\pi^\pm X} - \Delta\sigma_{\pi p\to\pi^\pm X} \tag{53}$$

obtained previously in a Regge-pole model based on ρ and ω universality.[22] This demonstrates once again the power of a topological analysis of hadron

cross sections.

Using Eqs. (42), (43), (51), and (52) one sees that Eq. (49) is automatically satisfied [in the sens that Eq. (49) becomes identical with Eq. (37)] and, using Eqs. (44) and (51), one sees that Eq. (50) is also automatically satisfied. The fact that the overall system of equations (31)–(38) and (47)–(50) is a compatible system is, of course, interesting. This simply means that SU(3) flavor symmetry is a perfectly acceptable property from the topological point of view. In fact SU(N) flavor symmetry is present in the theory of Ref. 6. It is also important to note that a coefficient -1 on the right-hand side of Eq. (38), suggested by the present data on $\Delta\sigma_{\pi p\to\pi^+ X}$, will destroy the compatibility of the above-mentioned system of equations. This is an additional reason for believing that these data are doubtful.

The previous considerations also clarify, we hope, the topological origin of the ρ and ω universality properties, which were used in the past as more or less *ad hoc* assumptions.

VII. CONCLUSIONS

One can conclude that the recent generalized DTU theory of Chew and Poenaru[6] leads, at its lowest-topological-entropy level, to a realistic description of an important piece of experimental data: differences of total and inclusive hadron cross sections. The data are sufficiently precise to test in an unambiguous manner our relations between hadron cross sections.

As discussed in Sec. IV our relations are derived directly from the theory of Ref. 6. The condition of the nonintersection of Landau lines and junction lines on the classical surface was crucial in the derivation of the relations discussed in Sec. IV A. We therefore expect these relations to be valid even at certain nonzero values of the topological entropy where the above-mentioned nonintersection still occurs. (More specifically we expect them to be valid at the so-called "parity-patched" planar level of Ref. 6.)

Our second set of relations (those of Sec. IV B) were based on the topological supersymmetry property, which we derived within the framework of the theory of Refs. 5 and 6 from a certain spin-momentum dependence which is valid only at zero entropy. Theoretically, these relations are expected to be violated by higher-order corrections.

Of course, we expect higher-order corrections to have important dynamical consequences, via a renormalization of propagators and couplings. However, the overall agreement of our zero-entropy relations with the experimental data suggests that these corrections are such that the scale imposed by the topological zero entropy on the amplitudes which are antisymmetric under crossing has to be globally preserved. The "primordial" world could well be a topological world.

We also showed that the topological supersymmetric structure of hadron cross sections has interesting consequences for Regge couplings. As a by-product of our study, we find a possible topological origin of the ρ and ω universality relations.

A topological description of hadron interactions in terms of two two-dimensional surfaces, the quantum surface and the classical surface, certainly shows great promise.

ACKNOWLEDGMENTS

One of us (B.N.) would like to thank Professor G.F. Chew for numerous correspondences and discussions over the last three years which had a big impact on the development of this paper. The authors are also indebted to Professor L.A.P. Balázs for a patient reading of the manuscript which had an influence on the ultimate construction of the paper. Finally, the authors would like to thank Professor V. Poenaru, Professor H.P. Stapp, Dr. U. Sukhatme, Dr. J. Uschersohn, and Professor R. Vinh Mau for penetrating and helpful remarks.

---

*Laboratoire associé au Centre National de la Recherche Scientifique.

[1]G. F. Chew and C. Rosenzweig, Phys. Rep. 41, 263 (1978).

[2]G. F. Chew, Nucl. Phys. B151, 237 (1979); Phys. Lett. 82B, 439 (1979).

[3]G. F. Chew, B. Nicolescu, J. Uschersohn, and R. Vinh Mau, CERN Report No. TH-2635, 1979 (unpublished).

[4]G. Veneziano, Nucl. Phys. B74, 365 (1974); Phys. Lett. 52B, 220 (1974).

[5]H. P. Stapp, Lawrence Berkeley Laboratory Reports Nos. LBL-10774, 1980 and LBL-11770, 1980 (unpublished).

[6]G. F. Chew and V. Poenaru, Phys. Rev. Lett. 45, 229 (1980); Z. Phys. C (to be published); and private communications.

[7]H. Harari, Phys. Rev. Lett. 22, 562 (1969); J. Rosner, *ibid.* 22, 689 (1969).

[8]J. G. Rushbrooke and B. R. Webber, Phys. Rep. 44, 1 (1978).

[9]G. C. Rossi and G. Veneziano, Nucl. Phys. B123, 507 (1976); see also L. Montanet, G. C. Rossi, and G. Veneziano, Phys. Rep. 63, 149 (1980).

[10]B. Nicolescu, in *Lecture Notes in Physics*, edited by

A. M. Saruis and H. Arenhövel (Springer, Berlin, 1981), Vol. 137.
[11]G. F. Chew and H. P. Stapp, private communication.
[12]H. J. Lipkin, Phys. Rev. Lett. 16, 1015 (1966); Phys. Rep. 8C, 175 (1973).
[13]P. G. O. Freund, Phys. Rev. Lett. 15, 929 (1965).
[14]V. Flaminio *et al.*, Reports Nos. CERN-HERA 79-01, 79-02, and 79-03 (unpublished).
[15]E. Beier *et al.*, Phys. Rev. D 17, 2864 (1978); 17, 2875 (1978).
[16]J. Whitmore, Phys. Rep. 27, 187 (1976).
[17]T. Fields and C. K. Chen, in *Nucleon-Antinucleon Interactions*, proceedings of the Stockholm Symposium, 1976, edited by G. Ekspong and S. Nilsson (Pergamon, New York, 1977), pp. 525-532.
[18]R. V. Gavai and D. P. Roy, Phys. Lett. 82B, 139 (1979); Nucl. Phys. B137, 301 (1978).
[19]S. N. Ganguli and D. P. Roy, Phys. Rep. 67, 201 (1980).
[20]B. Nicolescu, Nucl. Phys. B134, 495 (1978).
[21]K. Johnson and S. B. Treiman, Phys. Rev. Lett. 14, 189 (1965).
[22]H. J. Lipkin, Phys. Rev. D 5, 776 (1972).